

## INTERPRETING INFRARED COLOR-COLOR DIAGRAMS: CIRCUMSTELLAR DISKS AROUND LOW- AND INTERMEDIATE-MASS YOUNG STELLAR OBJECTS

CHARLES J. LADA

Harvard-Smithsonian Center for Astrophysics, 60 Garden Street, Cambridge, MA 02138

AND

FRED C. ADAMS

Department of Physics, University of Michigan, Ann Arbor, MI 48109

Received 1991 October 9; accepted 1992 January 10

### ABSTRACT

We investigate the behavior of well-established evolutionary classes of young stellar objects in the *JHK* infrared color-color diagram. We examine observations of classical and weak-line T Tauri stars, Herbig AeBe stars, infrared protostars, and classical Be stars. We find that the different types of objects tend to occupy well-defined and different regions of the color-color diagram and that to some degree the evolutionary nature of a YSO can be determined from its position in *JHK* color-color space. In an attempt to provide a physical explanation for the observed *JHK* colors of YSOs, we explore the behavior of circumstellar disk models in the color-color diagram. We find that the *JHK* observations of classical T Tauri stars with infrared excesses can be well explained by standard disk models in agreement with earlier studies. However, standard disk models cannot account for the large infrared excesses and the distribution of AeBe stars in the color-color diagram unless (1) these model disks contain central holes and (2) the basic physical parameters of the disks *always* conspire to produce temperatures at the inner edges of the disks in the narrow range between 2000–3000 K. The close correspondence between the deduced temperatures at the inner edges of the disks and the dust sublimation temperature suggests that dust is the primary source of opacity at infrared wavelengths in circumstellar disks around AeBe stars.

*Subject headings:* circumstellar matter — stars: pre-main-sequence

### 1. INTRODUCTION

The formation and early evolution of stars in our Galaxy occurs within the dense regions of molecular clouds. In this environment, young stellar objects (YSOs) are invariably associated with significant amounts of interstellar gas and dust which can absorb and reprocess a substantial fraction of the radiant energy emitted by the buried stars. As a result, the bulk of the luminous energy of a YSO is often radiated at wavelengths longward of  $1\ \mu\text{m}$ . Therefore, infrared observations are an essential and powerful tool for investigating star formation and early stellar evolution. Indeed, the structure of the circumstellar environment of a YSO can be deciphered from the shape of its infrared spectral energy distribution (SED) if sampled over a large enough wavelength range (e.g., 1–100  $\mu\text{m}$ ; Lada 1987, 1991). As a result, it has been possible to classify the infrared energy distributions of YSOs into a more or less continuous evolutionary sequence (from protostar to young pre-main-sequence star) which is well modeled by at least one physically self-consistent theory of star formation and early stellar evolution (Shu 1977; Adams, Lada, & Shu 1987, hereafter ALS; Shu, Adams, & Lizano 1987; Lada & Shu 1990).

However, obtaining sufficiently complete SEDs for a sufficiently large sample of young objects embedded in molecular clouds is a painstaking and time-consuming endeavor. It requires observations which are usually obtained at different telescopes with different angular resolutions and at different epochs of time. Given the possibility of YSO variability and source confusion that can arise with longest wavelength infrared observations (which are always made with large beams), interpretation of even the most complete infrared SEDs can often be difficult. The recent development of array

detectors at near-infrared wavelengths for astronomy (e.g., Wynn-Williams & Becklin 1987; Elston 1991) offers the promise of dramatically improving the current situation. Large-format infrared arrays allow the near-simultaneous multiwavelength observation of large populations of YSOs embedded in obscured clusters or buried throughout the entire extents of giant molecular clouds (e.g., De Poy et al. 1990; E. Lada et al. 1991; C. Lada et al. 1991; Gatley et al. 1991; Barsony, Shombert, & Kis-Halas 1991; Zinnecker, McCaughrean, & Wilking 1992). Although infrared arrays can provide observations of significantly large samples of embedded young objects for comparative study, the wavelength coverage of existing (large-format) arrays is relatively small (typically 1.25–2.2  $\mu\text{m}$ ). However, given the potential for advances in our understanding of star formation that can be gained by thorough study of large populations of embedded YSOs using infrared cameras, it is important to determine the extent to which useful information concerning the nature of embedded objects can be derived from near-infrared colors alone. Previous studies of *IRAS* observations have shown that useful information can be derived from analysis of a limited number of far-infrared colors (e.g., Emerson 1988; Hughes 1989). In this paper, we investigate the information content of observations obtained in the three standard near-infrared bands accessible with nearly all existing near-infrared arrays: *J* (1.25  $\mu\text{m}$ ), *H* (1.65  $\mu\text{m}$ ), and *K* (2.2  $\mu\text{m}$ ).

Early studies of infrared sources in the Chamaeleon dark cloud (Hyland 1981) and more recent observations of the obscured clusters in M17 (C. Lada et al. 1991) and Orion (Gatley et al. 1991) have suggested that useful information concerning the natures of YSOs can be inferred from observed *JHK* colors of groups of stars when such data are displayed in

the form of a color-color diagram (i.e., a plot of  $J-H$  vs.  $H-K$ , where  $J$ ,  $H$ , and  $K$  are in magnitudes). In particular, stars with intrinsic excess emission, heavily reddened stars, and stars with normal unreddened photospheric colors can be readily distinguished from each other on such plots. However, the degree to which a  $JHK$  color-color diagram is useful as a tool for investigating star formation directly depends on the extent to which the nature of an object can be derived from its position in  $JHK$  color-color space. It is clearly useful to address this question both empirically and theoretically. In § 2, we investigate the behavior of well-known types of YSOs on a  $JHK$  color-color diagram. In § 3, with the aid of circumstellar disk models, we attempt to provide a physical explanation for the observed behaviour of a subset of well-known YSOs (T Tauri stars and Herbig AeBe stars) in the  $JHK$  color-color diagram. We find that the pattern displayed by T Tauri stars in the  $JHK$  color-color diagram can be explained by invoking standard disk models to account for their  $JHK$  colors; this finding is consistent with previous interpretations of T Tauri stars as systems with circumstellar disks (Rucinski 1986; ALS; Adams, Lada, & Shu 1988, hereafter ALS 88; Beckwith et al. 1990; Adams, Emerson, & Fuller 1990 and others). On the other hand, standard disk models cannot explain the behavior of Herbig AeBe stars in the  $JHK$  color-color diagram, and from the color-color diagram we derive new insights into the physical nature of their circumstellar environments. Our study indicates that  $JHK$  colors alone can sometimes be very useful tools for studying star formation and early stellar evolution. The implications of our results are discussed in § 4. The main results of the paper are summarized in § 5.

## 2. BASIC OBSERVATIONAL DATA

In this section we investigate the behavior of well-known types of YSOs in the  $JHK$  color-color diagram. We consider the distribution of low-mass YSOs (i.e., classical T Tauri stars, weak-line T Tauri stars, and Class I sources), intermediate-mass YSOs (Herbig AeBe stars), luminous Class I sources (protostars?), and classical Be stars. Where possible we consider only observations obtained using the Arizona or Johnson photometric system (Johnson 1966; Koornneef 1983).

In Figure 1 we plot the distribution of low-mass YSOs within the Taurus-Auriga cloud complex on the  $JHK$  color-color diagram. The data are from the recent compilation by Kenyon & Hartmann (1992). Also plotted is the locus of points corresponding to the position of the *unreddened* main sequence. The colors for main-sequence stars are from Koornneef (1983) and correspond to the Johnson photometric system (Johnson 1966). The two parallel dashed lines form the reddening band for normal stellar photospheres. These lines are parallel to the reddening vector and bound the range in the color-color diagram within which stars with purely reddened normal stellar photospheres can fall. Crosses are positioned along each reddening line at positions corresponding to 5, 10, 15, 20, 30, and 40 magnitudes of visual extinction from their points of origin on the main sequence. The standard extinction law was assumed (e.g., Koornneef 1983).

The YSOs in Figure 1 are divided into three groups. Sources with a Class I designation were classified by Kenyon & Hartmann (1992) as such on the basis of their being deeply embedded (invisible) objects with infrared energy distributions steeply rising with wavelength. Most of these objects are likely to be protostellar in nature (e.g., Adams & Shu 1986; ALS). Classical

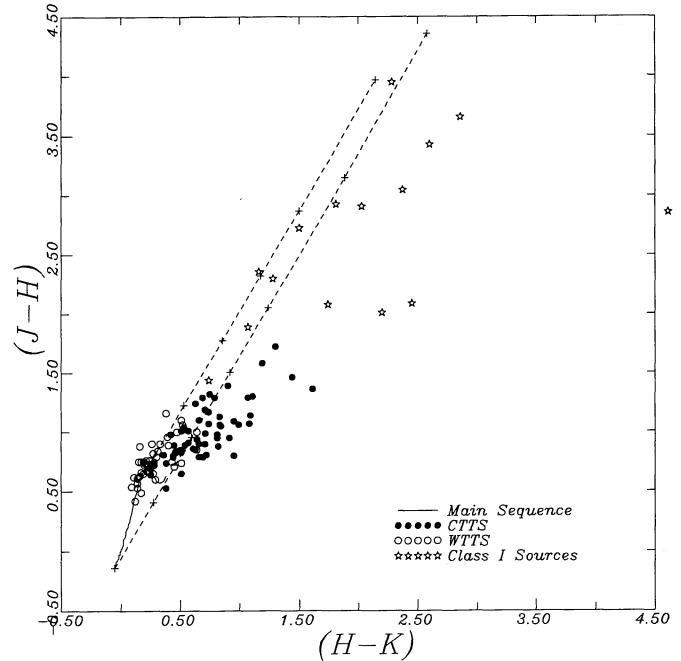


FIG. 1.—The  $JHK$  color-color diagram for low-mass YSOs in the Taurus-Auriga dark cloud complex. The data are taken from Kenyon & Hartmann (1992). The solid curve in the lower left-hand portion of the diagram is the locus of points corresponding to the unreddened main sequence. The two dashed lines which intersect the main-sequence curve near the minimum and maximum  $J-H$  values are parallel to the reddening vector. Crosses are plotted along each of these reddening lines at positions corresponding to 5, 10, 15, 20, 30 and 40 magnitudes of visual extinction from the points where they intersect the main-sequence curve. These two lines form the reddening band for normal stellar photospheres. Objects with colors that fall outside and to the right of this band are sources with intrinsic infrared excess emission. Class I sources, CTTS, and WTTS appear to be spatially segregated in the diagram. Class I sources occupy a region of the diagram characterized by very large values of extinction, while WTTS are located in the region corresponding to unreddened or only slightly reddened stars. CTTS lie between and are characterized by modest values of extinction. Moreover, the majority of Class I sources and CTTS display strong infrared excesses.

T Tauri stars (CTTS) are those objects from the Kenyon & Hartmann sample which have  $H\alpha$  emission line equivalent widths measured to be greater than  $10 \text{ \AA}$  (Herbig & Bell 1988). Weak-line T Tauri stars (WTTS) are those objects with  $H\alpha$  emission line equivalent widths of  $10 \text{ \AA}$  or less (Herbig & Bell 1988). The three groups of objects are well segregated on the color-color diagram. Class I sources lie in the region of the color-color plane characterized by large extinctions (i.e.,  $A_V \approx 10-40 \text{ mag}$ ) and for the most part lie outside and to the right of the reddening band, thus indicating the presence of intrinsic infrared excess emission. The scatter in the observations is also noticeably larger than that of the CTTS and WTTS. The CTTS and WTTS occupy a region of the diagram characterized by lower values of extinction (i.e.,  $A_V \approx 0-10 \text{ mag}$ ) than that occupied by Class I sources. The majority of stars classified as CTTS based on the equivalent widths of their  $H\alpha$  emission lie to the right of the reddening band; this location also indicates the presence of infrared excess emission. These objects are likely characterized by Class II SEDs (Lada 1987). The vast majority of the WTTS lie within the reddening band or along the main sequence, and they are likely Class III sources displaying no infrared excess at these wavelengths. We note that a

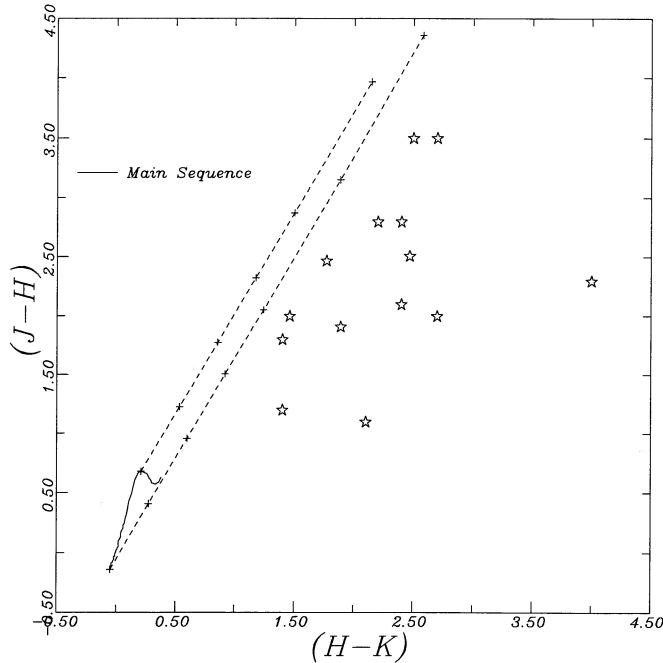


FIG. 2.—The  $JHK$  color-color diagram for luminous infrared protostars (Class I sources). The  $JHK$  colors of the luminous protostars are similar to those of the low-luminosity Class I sources in Figure 1, except for the fact that the colors of *all* the luminous Class I sources are characterized by strong infrared excess at these wavelengths.

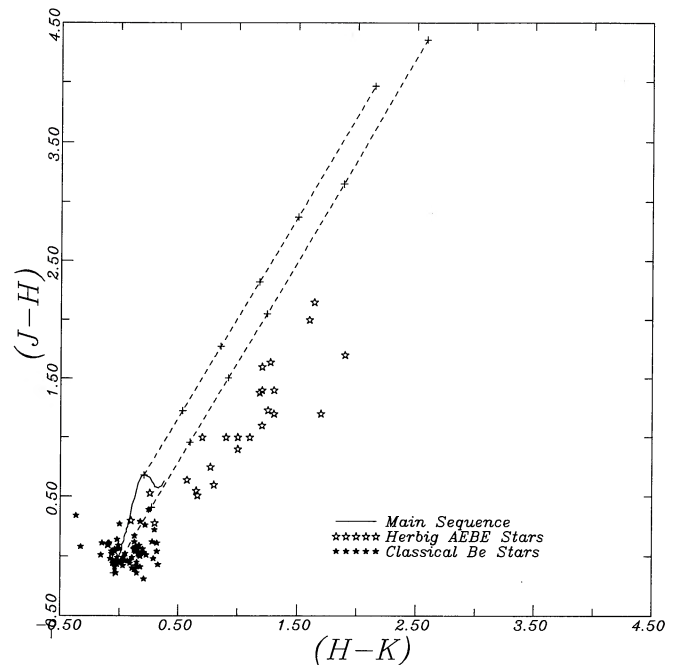


FIG. 3.—The  $JHK$  color-color diagram for Herbig AeBe stars and classical Be stars. These two groups of stars are clearly spatially segregated on the diagram. Herbig AeBe stars have colors which overlap with luminous protostars at the upper end and CTTS at the lower end of their distribution in color-color space. However, AeBe stars generally display much greater infrared excesses than do CTTS.

significant number of CTTS lie within the reddening band and even overlap with some of the WTTS. This result does not necessarily mean that these CTTS lack infrared excesses; to determine whether or not these stars have infrared excess requires additional and precise knowledge of either the extinction to the stars or their underlying spectral types.

In Figure 2 we plot the distribution of luminous protostellar candidates (Class I sources) in the  $JHK$  color-color diagram. The sources were selected from the Wynn-Williams (1982) compilation. The observations were taken from the infrared catalog of Gezarin, Schmitz, & Mead (1987). All sources with  $JHK$  measurements were plotted. All the luminous Class I sources lie high up and well to the right of the reddening band with a dispersion comparable to the low-luminosity Class I sources of Figure 1. Similar to their low-luminosity counterparts, these sources are characterized by large extinctions and large infrared excesses and occupy a region of the color-color diagram clearly distinct from CTTS and WTTS.

In Figure 3, we plot the distributions of Herbig AeBe stars and classical Be stars on the  $JHK$  color-color diagram. The data for the Herbig AeBe stars are from the compilation of Finkenzeller & Mundt (1984) and those for the field Be stars are from Ashok et al. (1984). Herbig AeBe stars and classical Be stars are clearly differentiated on the  $JHK$  color-color diagram, a trend which has been observed in other comparisons of the colors of these two classes of stars (e.g., Finkenzeller & Mundt 1985; Mendoza 1987). Classical Be stars are concentrated in a relatively localized region at the blue end of the main sequence. These stars show little evidence of being reddened but in many cases exhibit infrared excesses. Herbig AeBe stars, on the other hand, have a more extended distribution and are located in a band which is displaced from (but

more or less parallel to) the reddening band for normal stars. For the most part AeBe stars appear to be characterized by large amounts of reddening and they exhibit substantial excess infrared emission. Comparison of Figures 2 and 3 shows that the upper end of the band of Herbig AeBe stars significantly overlaps with the lower end of the band of infrared protostars. Thus, the near-infrared colors of luminous infrared protostars (Class I sources) are not much different from those which would be predicted for extremely reddened AeBe stars. The protostellar envelopes which produce the deep silicate absorption features and large excesses at mid- and far-infrared wavelengths in the SEDs of typical Class I sources (e.g., Adams & Shu 1986; ALS; Lada 1991) could easily produce the additional extinction necessary to shift an AeBe star into the heart of the protostellar band on the  $JHK$  color-color diagram. At the lower end of the AeBe band, AeBe stars overlap somewhat with CTTS. However, AeBe stars are systematically more displaced from the reddening band than are CTTS, as careful comparison of Figures 1 and 3 shows.

### 3. INTERPRETATION

#### 3.1. Standard Disk Models

Comparison of Figures 1–3 shows that YSOs of different types tend to occupy different regions of the  $JHK$  color-color diagram. This finding suggests that the nature of a YSO as a protostar, AeBe star, classical Be star, CTTS, or WTTS can indeed be estimated from its position in  $JHK$  color-color space, and that the  $JHK$  color-color diagram is potentially a useful tool for investigating star formation. To fully exploit the information contained in this diagram, we now attempt to provide a physical interpretation for the behavior of the

various types of young objects when plotted in  $JHK$  color-color space. Normal stellar photospheres (including those of classical pre-main-sequence stars) have colors which place them either on the main-sequence line or in the reddening band. For a star to be displaced to the right of its main-sequence position or the reddening band requires the presence of infrared emission in excess of that normally emitted in the star's photosphere. For a star to appear to the left of the main sequence or the left boundary of the reddening band would require physically implausible conditions. The upper left part of the  $JHK$  color-color diagram can therefore be considered a forbidden region for young stellar objects. To produce near-infrared excess emission around a single star requires the existence of substantial amounts of circumstellar material located relatively close to the stellar surface. In principle this material could be distributed in any number of different ways around the star. However, for visible stars such as CTTS and AeBe stars, excess emission is observed over a large range of wavelengths from the near-infrared to the millimeter regions of the spectrum. The amount of circumstellar material needed to produce the observed excess over this large wavelength range is so great that, if distributed in a spherical manner around the star, it would extinguish the star from detection at visible and even near-infrared wavelengths. Consequently, in such objects the material producing the excess emission is generally thought to be contained in a highly flattened, stable structure, such as a disk. Indeed, the broad-band energy distributions of CTTS have been very successfully modeled with circumstellar disks in numerous investigations (e.g., Rucinski 1985; ALS; Beal 1987; ALS 88; Kenyon & Hartmann 1987; Beckwith et al. 1990; Adams et al. 1990, etc.).

In order to explore the extent to which standard disk models can reproduce the observed patterns of  $JHK$  colors for young stellar objects with infrared excesses, we have used the numerical code described by ALS88 to compute a set of standard circumstellar disk models. Our standard disk is a spatially thin, optically thick disk with a radial extent of 100 AU surrounding a central star of specified surface temperature  $T_*$ . The luminosity of the disk derives from both reprocessed stellar light and intrinsic disk emission. The radial temperature distribution in the disk results from an appropriate combination of the energy input from reprocessing and intrinsic disk luminosity. The component of the radial temperature gradient resulting from reprocessing stellar light is calculated as described by ALS88 and Adams & Shu (1986) and is the same for all models and has the approximate form  $T(r) \propto r_D^{-0.75}$ . The component of the radial temperature gradient resulting from the intrinsic luminosity in the disk is prescribed to be of the form  $T(r) \propto r_D^{-q}$ . The power-law index  $q$  is a parameter which is varied between the various models. The ratio,  $f_{\text{Disk}}$ , of the intrinsic disk luminosity,  $L_{\text{Disk}}$ , to total system luminosity (star + disk),  $L_{\text{Total}}$ , is one of the parameters necessary to completely specify a model. The other necessary parameters are  $\theta$ , the inclination of the disk to the observer,  $T_*$ ,  $q$ , and  $L_{\text{Total}}$ . To determine the extent to which model disks could populate  $JHK$  color-color space, we computed 18 separate models covering the full range of possible inclinations ( $\cos \theta = 1.00, 0.866, 0.707, 0.50, 0.25, 0.10$ ) and temperature indices ( $q = 0.75, 0.67, 0.50$ ) for each combination of  $T_*$ ,  $L_{\text{Total}}$ , and  $L_{\text{Disk}}$  that we considered. Models were run for central stars with temperatures of 3000, 4000, 5000, 7000, 9000, and 12,000 K to span the appropriate range of surface temperatures of observed YSOs. The total system luminosity was chosen to be either  $3 L_\odot$  or  $500 L_\odot$  depending

on the temperature of the central star. However, this parameter has negligible effect on the calculated colors. In Figure 4 we show the locations occupied by model stars surrounded by standard circumstellar disks. Figure 4a illustrates the extent of  $JHK$  color-color space occupied by standard disk models in which the disk has an intrinsic luminosity equal to  $0.1 L_{\text{Total}}$ . The models are tightly clustered but clearly fall outside the reddening band in the region of infrared excess as expected. For a given  $T_*$ , the variation in inclination accounts for the bulk of the dispersion in  $JHK$  colors displayed by the models, the effect of variations in the temperature index  $q$  is much less significant. The close proximity of the 5000 and 12,000 K models reflects the fact that at these and higher temperatures the  $JHK$  fluxes of the stars are near the Rayleigh-Jean's portion of the stellar SEDs. Increasing the relative fraction of intrinsic disk luminosity ( $f_{\text{Disk}}$ ) has the effect of slightly displacing and spreading out the distribution of models in the diagram in a manner similar to what one would expect if the sources were somewhat reddened. However, even in the extreme case where most of the system luminosity originates in the disk, Figure 4b, the area of the  $JHK$  color-color plane filled by disk models only slightly increases. We note that because we model the central stars as blackbodies, the models do not accurately represent true stellar colors. In general model stars tend to have redder  $HK$  colors and bluer  $JH$  colors than true stars. The discrepancy between blackbody and stellar colors begins to be noticeable on the  $JHK$  color-color diagram for model stars with effective temperatures in the range between 3000 and 7000 K and is significant for stars with temperatures between 3500 and 5000 K. In the Appendix we discuss the magnitude of this discrepancy and present examples of models which have been adjusted to correct for this effect and more closely mimic true stellar colors.

Figure 5 compares the locations of a set of standard disk models for stars with  $T_* = 3000$  K with the distribution of CTTS on the color-color diagram. The unextincted standard models clearly form an outer boundary to the extent of observed CTTS in the infrared excess region. Moreover, the figure clearly shows that with the introduction of some external reddening, the disk models can account for most of the observed spread in the  $JHK$  colors of CTTS in the infrared excess region. For example, in Figure 5 the location of a set of standard models with  $f_{\text{Disk}} = 0.1$ ,  $T_* = 3000$  K and an external extinction of  $A_V = 3.0$  magnitudes is indicated. With extinctions between 0 and 4.0 magnitudes such models could readily account for majority of the CTTS located outside the reddening band. As shown in the Appendix, models with higher temperature central stars could also fit these observations if similar extinctions were allowed. However, upon closer inspection of Figure 5, it is also evident that to account for the stars with the largest infrared excesses requires models in which a large fraction of the system luminosity resides in the disk. Not surprisingly, these particular stars mostly turn out to be "flat" spectrum T Tauri stars (e.g., T Tauri, DG Tau, HL Tau) for which previous spectral modeling has already indicated large intrinsic disk luminosities (ALS88). Application of standard disk models to the analysis of the  $JHK$  color-color diagram for CTTS indicates that the manifestation of infrared excess in  $JHK$  color-color space can be well accounted for by the presence of circumstellar disks in these systems. This conclusion appears to be borne out by recent modeling of disk atmospheres by Calvet et al. (1992), who find that the presence of disks around stars with effective temperatures between 4000

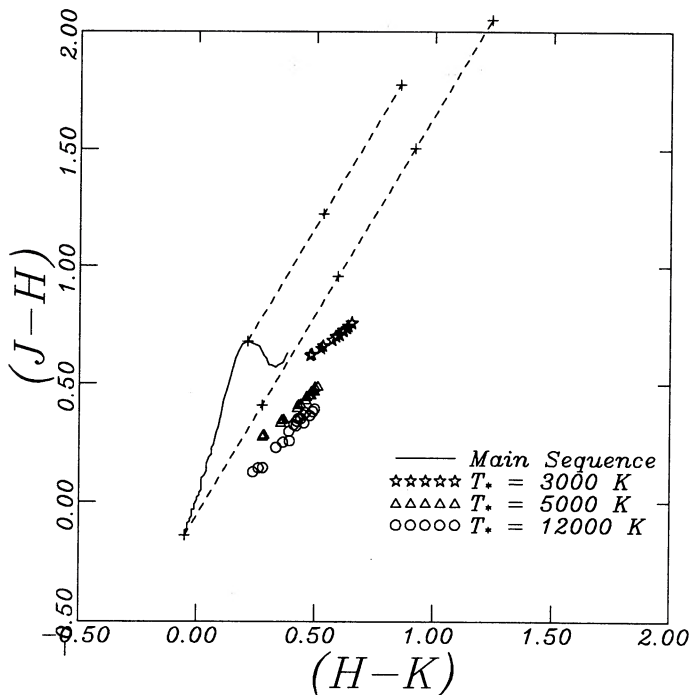


FIG. 4a

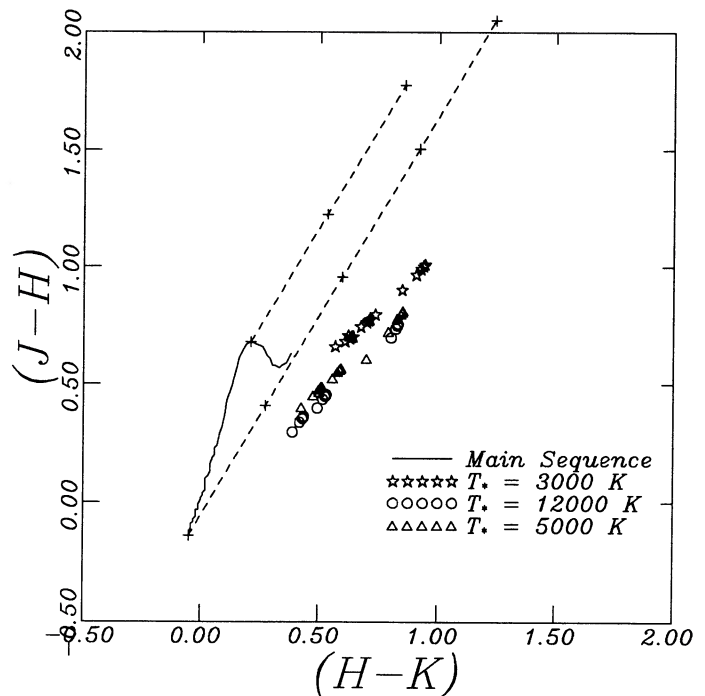


FIG. 4b

FIG. 4.—The *JHK* color-color diagrams for model YSOs with standard circumstellar disks. Models are plotted for central stars with three different surface temperatures, 3000, 5000, and 12,000 K. For each temperature star a grid of 18 models is plotted corresponding to luminous disks with six different line-of-sight inclinations ( $\cos \theta = 1.00, 0.866, 0.707, 0.50, 0.25,$  and  $0.10$ ) for each of three different temperature power-law indices ( $q = 0.75, 0.67,$  and  $0.50$ ; see text). The uppermost point of each grid in the color-color diagram typically corresponds to a disk with  $\cos \theta = 1.00$  and  $q = 0.5$ , while the lowermost point corresponds to a model with  $\cos \theta = 0.10$  and  $q = 0.75$ . (a) The color-color diagram for systems whose circumstellar disks intrinsically generate 10% of the total system (star + disk) luminosity. (b) The color-color diagram for models whose circumstellar disks intrinsically radiate 90% of the total bolometric or system luminosity. The total luminosity ( $L_{\text{bol}}$ ) was  $500 L_{\odot}$  for models with a 12,000 K central star and  $3 L_{\odot}$  for models with 5000 K and 3000 K central stars.

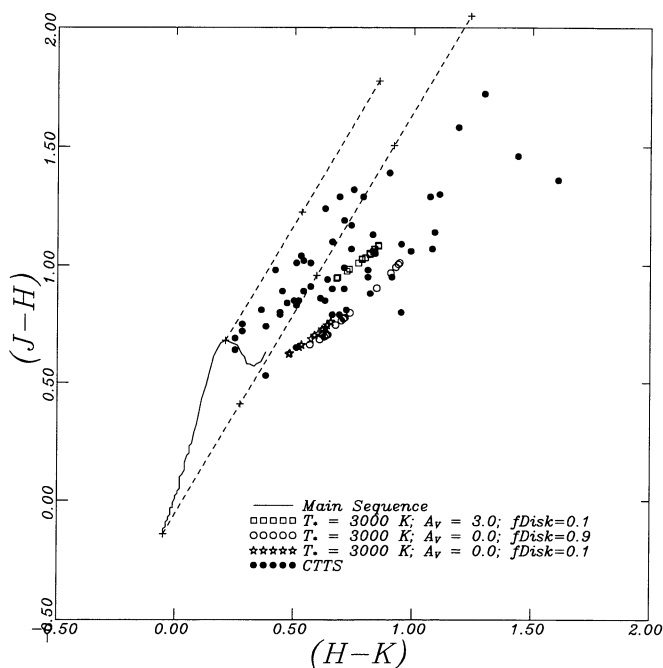


FIG. 5.—Comparison of the distributions of CTTS and standard disk models on the *JHK* color-color diagram. Three different (18) model grids are plotted for systems with a 3000 K central star. Systems with  $f_{\text{Disk}} = L_{\text{Disk}}/L_{\text{Total}} = 0.1$  and  $A_V = 0.0-3.0$  can account for the observed colors of most CTTS located outside the reddening band. Model disks with higher values of  $f_{\text{Disk}}$  (e.g.,  $f_{\text{Disk}} = 0.9$ ) are needed to account for the CTTS with the largest infrared excesses and displacements from the reddening band.

and 5000 K can account for the near-infrared colors of 80% of CTTS. Presumably, allowance for variation in extinction and lower stellar effective temperatures would enable the Calvet et al. models to account for an even larger fraction of CTTS colors. Thus our finding is in accord with the now generally accepted interpretation of T Tauri star systems.

Figure 6 compares the distribution of Herbig AeBe stars with standard disk models for an appropriately hotter central star ( $T_{\star} = 12,000$  K). Unlike the case for the CTTS, standard disk models *fail* to account for the *JHK* colors of most AeBe stars, even when relatively large amounts of extinction are invoked. Indeed, the standard models appear to form an inner boundary to the band of observed AeBe stars in the infrared excess region! AeBe stars clearly exhibit larger infrared excesses than can be accounted for in standard disk models. This result obtains even when the disk luminosity is a substantial fraction of the total system luminosity, as a comparison of Figures 6 and 4b will indicate. Moreover, the extent of the observed AeBe star band along the reddening vector requires uncomfortably large extinctions (i.e.,  $A_V \approx 7-10$  mag) for the standard models.

What is the cause of the large displacement of AeBe stars from the reddening band? The presence of excess emission over a large range of wavelengths in these stars still suggests a disk model. How is it possible to preserve the disk model to account for the long-wavelength emission in the energy distributions and at the same time explain the anomalous *JHK* colors of these stars? If circumstellar disks are the cause of the excess in AeBe stars, then the shapes of their SEDs must differ from

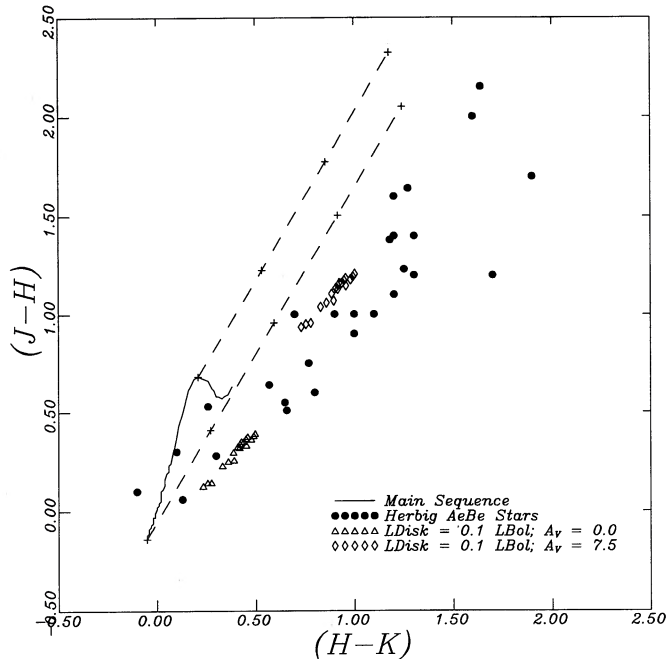


FIG. 6.—Comparison of the distributions of Herbig AeBe stars and standard disk models on the  $JHK$  color-color diagram. Two model grids are plotted for systems with a 12,000 K central star and  $f_{\text{Disk}} = 0.1$  but with differing foreground extinctions. Unlike the CTTS, AeBe stars display infrared excesses which are significantly larger than can be produced by the standard models.

those of the standard disk models and CTTS. Indeed, the large displacement of the AeBe stars from the reddening band requires a spectral energy distribution whose slope is consistent with that of a reddened or unreddened standard disk model between  $J$  and  $H$  but at the same time is “redder” or less steeply falling between  $H$  and  $K$  than that of the same reddened or unreddened disk model. Recent analysis of AeBe star energy distributions by Hillenbrand et al. (1992) has shown that the energy distributions of at least some AeBe stars do indeed exhibit such a characteristic. They suggest, as we also demonstrate below, that such an effect could be produced by a disk with a central hole.

### 3.2. Disk Models with Central Holes

In Figure 7 we plot the SEDs of a series of circumstellar disk models with and without holes around a 12,000 K star. The disk models with holes were straightforwardly computed by modifying the standard disk models to turn off the contributions of all disk emission (i.e., reprocessing and intrinsic) to the emergent spectrum for those portions of the inner disk where the disk temperature exceeded a specified value,  $T_D$ . Since the surface temperature of the disk,  $T(r)$ , is roughly proportional to  $r^{-q}$ , the size of the hole scales with the adopted cutoff temperature for a fixed power-law index  $q$  and a fixed total system luminosity. In addition the removal of disk emission in the region of a hole results in a decrease in the intrinsic disk and total system luminosities from the initial parameterized values (in this example,  $50 L_{\odot}$  and  $500 L_{\odot}$ , respectively). Figure 7 shows that introducing a central hole in a disk model produces a dip in the SED at near-infrared wavelengths which is absent in the SED of the models without a hole. This produces the desired effect of creating a flatter SED slope between  $H$  ( $1.65 \mu\text{m}$ ) and

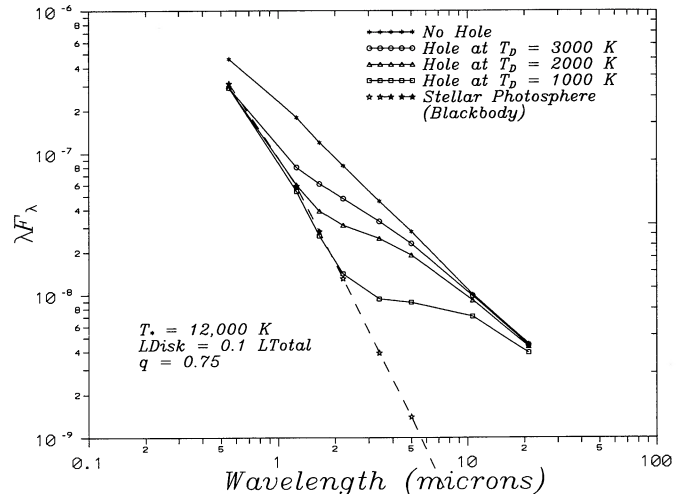


FIG. 7.—Spectral energy distributions (SEDs) for disk models with and without central holes around a star with a 12,000 K surface temperature. The models were calculated assuming a distance to the model systems of 160 pc, an initial total system luminosity of  $500 L_{\odot}$ , and a disk inclination of  $\cos \theta = 0.707$ . Also plotted for comparison is the SED for a 12,000 K star without a disk. For these models, the size of the hole increases with decreasing inner disk temperature  $T_D$ . In addition, the total system luminosity decreases from the initial parameterized value ( $500 L_{\odot}$ ) in response to the removal of intrinsic disk luminosity from the region of the hole.

$K$  ( $2.2 \mu\text{m}$ ) than could be produced by the amount of extinction necessary to account for the slope between  $J$  ( $1.25 \mu\text{m}$ ) and  $H$ . Yet, at longer infrared wavelengths, substantial excess emission is still evident as comparison with the SED from a diskless stellar photosphere shows.

To investigate the effect of central holes on the appearance of disk systems in the  $JHK$  color-color diagram we plot six different disk models with holes in Figure 8. This figure shows that the introduction of central holes in the standard models has a profound effect on the appearance of the color-color diagram. Models with holes are capable of populating a much larger fraction of the diagram than standard disk models. Moreover, the position of a model disk in color-color space is much more sensitive to parameters such as disk inclination, temperature index, and, in particular, fractional disk luminosity, than in the standard models without holes. As can be expected, the size of the central hole has the most significant effect on determining the distribution of model colors in the color-color diagram. For example, the hole can always be made large enough (i.e., with a low enough inner disk temperature) that the disk radiates negligibly at  $JHK$  wavelengths. The models would then collapse to a single degenerate point on the main-sequence locus. The hole can also be made sufficiently small that the disk dominates the emission at  $J$ ,  $H$ , and  $K$  in which case the models would be indistinguishable from the standard models of Figure 4. Between these two extremes, however, the  $JHK$  colors of such systems are very sensitive to the temperature at the inner edge of the disk; this temperature in turn depends on both the nature of the disk and the size of its hole.

Comparison of Figures 8 and 6 shows that, unlike the standard disk models, disks with holes actually have a larger dispersion on the  $JHK$  color-color diagram than that of observed YSOs. Consequently, the data can meaningfully constrain the models. Figure 9 shows a comparison of the distributions of AeBe stars with a subset of model disks with central holes

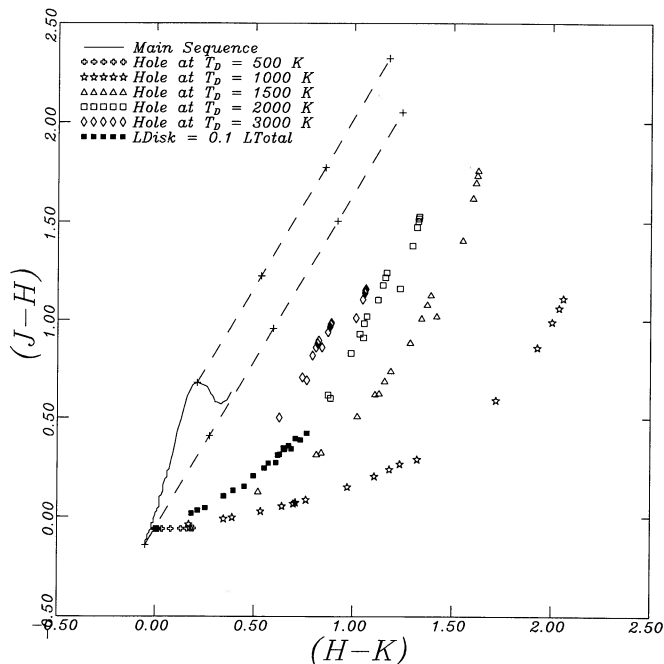


FIG. 8.—The color-color diagram for intrinsically luminous (i.e.,  $f_{\text{Disk}} = 0.9$ ) model disks with central holes of varying size around a 12,000 K star. Also plotted is a grid of models with relatively low intrinsic luminosity ( $f_{\text{Disk}} = 0.1$ ) and a hole at whose edge the disk temperature is 2000 K. See text for discussion. Other model parameters (i.e.,  $q$ ,  $\cos \theta$ ) are similar to those of Fig. 4.

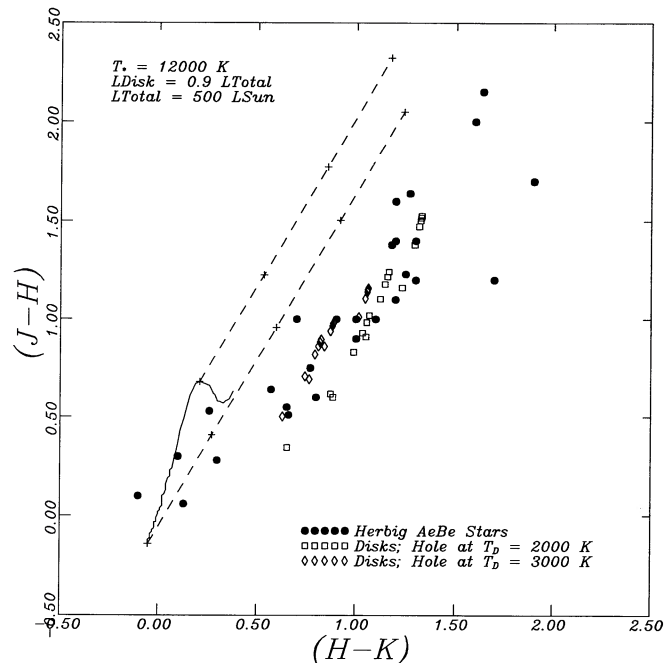


FIG. 9.—Comparison of the distributions of AeBe stars and those model disks that best match the observed data on the  $JHK$  color-color diagram. The observations are well fitted by model disks with central holes provided that the disk temperature at the edge of the holes is in the narrow range between 2000 and 3000 K.

which best fit the observations. These disk models contain holes in a relatively narrow range of inner disk temperature (i.e., in the range 2000–3000 K) and also have relatively high (initial) intrinsic disk luminosities (i.e.,  $L_{\text{Disk}} = 0.9 L_{\text{Total}}$ ). Comparison with Figure 8 indicates that disks with holes and only slightly lower inner temperatures do not fit the observations. Disks with somewhat higher inner temperatures also fail to fit the observed points. Model disks with low intrinsic disk luminosities (i.e.,  $L_{\text{Disk}} = 0.1 L_{\text{Total}}$ ) also do not fit the data unless these disks both have holes in exactly the same temperature range and are reddened on average by 5–7 mag of visual extinction. Purely reprocessing disks with similar holes could fit the observations only if dimmed by even larger amounts of extinction.

Although the AeBe star data provide strong constraints on the inner disk temperatures, they do not constrain other disk parameters such as the intrinsic disk luminosity as strongly because of the possible uncertainty in the amount of extinction that exists toward the sources in the observed sample. The physical sizes of the holes in the models are also not as strongly constrained, since they depend on the dust temperature distribution in the disks, the total system luminosity, and the fractional intrinsic disk luminosity. For disks with holes and inner temperatures between 2000 and 3000 K, the inner radii of the holes can range anywhere between 4 and 35 stellar radii for a 12,000 K central star and a total system luminosity of  $500 L_{\odot}$ . The smaller values correspond to systems with little or no intrinsic disk emission, and the larger values to systems with large relative disk luminosities. Stars with lower temperatures and systems with lower total luminosities also tend to have much smaller holes for the same range of inner disk temperatures.

In summary, the preceding analysis suggests that the  $JHK$  colors of Herbig AeBe stars can be fitted by a wide variety of disk models provided that (1) these model disks contain central holes and (2) that the basic physical parameters characterizing the disks and their central stars (i.e., luminosity, extinction, stellar surface temperature, disk temperature law, hole radius, etc.) *always* conspire to produce inner disk temperatures in the narrow range 2000–3000 K.

#### 4. DISCUSSION AND IMPLICATIONS

Analysis of the  $JHK$  color-color diagrams for well known YSOs appears to provide interesting insights into their nature. In particular, for AeBe stars, we find the unanticipated result that their locations in  $JHK$  color-color space require disk models with central holes if disks are the cause of their excess infrared emission. Moreover, the only disk models which fit the data are those in which the disk temperature at the radius of the hole is in the relatively narrow temperature range of 2000–3000 K. This result is very robust in the sense that it is essentially independent of other model parameters such as the disk luminosity, stellar luminosity, radius of the hole, surface temperature distribution of the disk, etc. This finding suggests a common underlying physical explanation. In this context, therefore, we take special note of the coincidence between the derived inner disk temperatures and the sublimation temperature of interstellar dust, roughly 2000 K (B. Draine 1992, personal communication). The obvious interpretation of our result is that dust provides the primary source of opacity in circumstellar disks. The inferred holes in the disks around AeBe stars are thus actually holes in the distribution of circumstellar dust. Whether or not there is an absence of all material

in the holes is not discernible from the observations modeled here. The holes could be filled with optically thin gas which extends all the way to the surfaces of the central stars. In this case much of the stellar activity observed at optical wavelengths (e.g., variability, emission lines, etc.) could still be due to some process of disk accretion as is often assumed (Strom et al. 1992).

However, the presence of such opacity holes would place constraints on the surface density of disk material within the holes and consequently on the possible rate of accretion of any material through the hole. For example, the condition for optically thin disk gas is  $\kappa\Sigma < 1.0$ , where  $\kappa$  is the appropriate gas opacity coefficient. From the low-temperature opacity tables of Alexander, Johnson, & Rypma (1983), we estimate that the inner disk will be optically thin if  $\Sigma$  is less than 250–1000  $\text{g cm}^{-2}$  for the temperature range 2000–3000 K. The mass accretion rate through the hole is given by  $\dot{M} = 2\pi R_H \Sigma v_r$ . For a typical hole radius,  $R_H$ , of  $3 \times 10^{12}$  cm, a radial accretion velocity,  $v_r$ , comparable to the speed of sound (i.e.,  $\approx 3 \text{ km s}^{-1}$ ), and  $\Sigma \leq 250 \text{ g cm}^{-2}$ ,  $\dot{M} \leq 2 \times 10^{-5} M_\odot \text{ yr}^{-1}$  if the material is to remain thin. Moreover, if the mass of the disk could be independently obtained (using millimeter-wave observations for instance), then the existence of a hole at the dust destruction radius would constrain how this mass was radially distributed through the disk. For a power-law radial surface density distribution of the form  $\Sigma(r) = \Sigma_H (r/R_H)^{-p}$ ,

$$\Sigma_H = \frac{(2-p)M_D}{2\pi R_H^2 [(R_D/R_H)^{2-p} - 1]}.$$

For a disk size,  $R_D = 100 \text{ AU}$ , and a disk mass,  $M_D = 0.25 M_\odot$ , appropriate for an AeBe star (e.g., Natta et al. 1992),  $p < 0.5$  would give a surface density  $\Sigma_H < 1170 \text{ g cm}^{-2}$ . We note that the values of  $p$  and  $\dot{M}$  we have just estimated should be regarded with caution, since they depend sensitively on the assumed opacities which may be highly uncertain. However, these examples serve to illustrate how the existence of inner disk holes could be used to derive important information concerning the physical properties of circumstellar disks around YSOs.

If the above interpretation is correct and if dust provides the opacity in circumstellar disks and its sublimation produces holes in the inner disk, then such holes should also exist in the disks of the CTTS. Yet, the *JHK* observations of most CTTS can be well fitted by the standard (hole-less) disk models. The reason for this apparently paradoxical situation is simply that the temperatures of these stars are much closer in value to the dust sublimation temperature than those of AeBe stars. Consequently, the dust destruction radius is expected to be much closer to their surfaces, and the inner holes are relatively small in size (i.e.,  $1-3 R_*$ ). Therefore, the *JHK* colors of a T Tauri star system with a disk hole at 2000 K are little different from a system containing a circumstellar disk without a hole. Moreover, for CTTS the *J*, *H*, and *K* bands are very close in wavelength to the peak in the stellar energy distribution. In this wavelength regime, the precise values of the stellar surface temperature and extinction have greater effect on the shape of the emergent energy distribution than the presence of a hole in the disk inward of the dust destruction radius. Nonetheless, observations of some CTTS at longer wavelengths have suggested the presence of inner holes. From comparison of  $12 \mu\text{m}$  and near infrared fluxes Beckwith et al. (1990) argued for the pres-

ence of disk inner holes with sizes  $\approx 0.05 \text{ AU}$  around a number of CTTS they studied. This size scale is very close to the sizes our models give for dust destruction holes around typical CTTS. The hypothesis that dust is the source of opacity in circumstellar disks around YSOs and its destruction results in creation of inner dust “holes” is consistent with the *JHK* data of both CTTS and Herbig AeBe stars. Of course we cannot be certain that circumstellar disks with dust holes provide a unique explanation for the *JHK* colors of AeBe stars. Whether or not different modifications of the standard disk model or an entirely different class of physical models can be constructed to account for these observations is as yet unclear.

Another interesting aspect of the comparison of disk models to the *JHK* observations of AeBe stars is that the observations are more readily fitted by disks with relatively high intrinsic luminosities. A similar result was recently obtained from detailed model fits to the complete energy distribution of the AeBe star LHa 198 where nearly half the luminosity of the system was determined to originate in its circumstellar disk (Natta et al. 1992). As mentioned earlier, this result is not unique in the sense that disks with relatively low intrinsic luminosities or even purely reprocessing disks could also fit the data if substantial amounts of foreground extinction (i.e.,  $A_V \approx 7 \text{ mag}$  or greater) exist toward typical AeBe stars. Although estimating extinction toward such stars is not straightforward, Finkenzeller & Mundt have derived extinctions for roughly 60% of known AeBe stars from the *B-V* colors and spectral types. The average extinction toward these AeBe stars is  $1.9 \pm 1.0 \text{ mag}$ . This is significantly less than what would be required for purely reprocessing models to fit the data in the color-color diagram. If this estimate is correct, then our analysis of the color-color diagram suggests that the disks around AeBe stars are intrinsically luminous. From our models and the *JHK* colors alone we cannot determine precisely how luminous these disks actually are; however, our analysis does suggest that *the intrinsic disk luminosities could be comparable to those of the central stars*. If intrinsic disk emission contributes significantly to the luminosity of an AeBe star then the observed bolometric luminosity of the system must at least exceed that of a main-sequence star of similar spectral type. In this context we note that Finkenzeller & Mundt determined lower limits for the luminosities of AeBe stars by integrating their optical-infrared energy distributions without correcting for reddening. They found that the luminosities of the vast majority of these stars are *greater* than the luminosities of main-sequence stars of similar spectral type, placing these stars well *above* the main sequence on the H-R diagram (Finkenzeller & Mundt 1985; see their Fig. 6). Furthermore, if the energy distributions of these stars are corrected for the extinctions estimated by Finkenzeller & Mundt, the dereddened luminosities place them very close to the recently calculated theoretical birthline for intermediate mass stars (Palla & Stahler 1990; see their Fig. 3). If the extinctions to these stars were as large as needed for reprocessing disks or low luminosity disks to fit the *JHK* colors, then these stars would clearly fall well *above* the theoretical birthline. But this could occur only if the bulk of the luminosity from these systems were generated in the disks and not in the stars. The above arguments favor an interpretation in which the locations of AeBe stars high along the reddening line in the *JHK* color-color diagram are the result of their disks being intrinsically luminous rather than the result of large foreground extinctions toward the stars.

If correct, this interpretation has important implications. In particular, it requires that AeBe stars are surrounded by very active accretion disks and consequently must be very young. To produce a significant amount of luminosity (e.g.,  $100 L_{\odot}$ ) via disk accretion would require relatively high accretion rates (e.g.,  $\approx 5 \times 10^{-6} M_{\odot} \text{ yr}^{-1}$ ) for a typical AeBe star. However, if the accretion rate becomes too high, it would be difficult to maintain a low enough gas opacity in the inner disk regions to create observable holes. Definitively demonstrating whether or not a significant fraction of the observed luminosity of an AeBe star originates in its circumstellar disk is clearly an important next step for future studies of these objects.

Earlier we noted that luminous protostars had *JHK* colors which appeared to be similar to those which are expected from heavily reddened AeBe stars. In addition, protostars have been shown to exhibit spectral features (e.g., calcium infrared triplet emission lines) in the near-infrared very similar to those of AeBe stars (McGregor, Persson, & Cohen 1984). It is possible, therefore, that at the heart of luminous protostars are stellar systems very similar to AeBe stars and that AeBe stars are protostellar objects very recently stripped of their protostellar envelopes. We also point out, however, that the dispersion of protostars on the color-color diagram is larger than that of AeBe stars. The larger dispersion of protostellar sources is likely related to their substantial circumstellar envelopes rather than differences in the structures of their circumstellar disks. The extinction through protostellar envelopes can be so large that scattering can be important at near-infrared wavelengths. Evidence for scattered light at near-infrared wavelengths has been noted in the energy distributions of a number of Class I sources (ALS). The effect of scattering would cause a blueward shift of the short-wavelength colors and could result in a larger dispersion of colors in the *JHK* color-color diagram. To fully understand the behavior of protostars and other heavily embedded objects on the *JHK* color diagram will require modification of YSO models to include the effect of scattering.

Finally, we noted earlier that classical Be stars have *JHK* colors which are clearly distinct from AeBe stars. Indeed comparison of Figures 3 and 4 shows that the infrared excesses of classical Be stars cannot be explained by standard disk models. However, comparison with Figure 8 suggests that they can be fitted by disks with holes corresponding to inner temperatures which are quite low (e.g.,  $T_D \approx 500$  K). Clearly, these holes correspond to temperatures much lower than the dust destruction temperature and destruction of dust cannot explain their sizes. Interestingly, studies of the energy distributions of Be stars suggest that the source of their infrared excesses is free-free emission (Gehrz, Hackwell, & Jones 1974) from a disk in which free-free absorption and not dust is not the main source of opacity (Lamers 1987). These studies indicate that the disks are optically thin out to a wavelength of about  $7 \mu\text{m}$ ; this result is consistent with the lower inner disk temperatures we infer here. The disks around classical Be stars are smaller and considerably less massive than the disks around AeBe stars. Whether they represent a more advanced stage of AeBe star evolution or a totally unrelated phenomenon is unclear from the *JHK* data alone.

## 5. SUMMARY

The main results of our analysis of the *JHK* infrared color-color diagram for young stellar objects can be summarized as follows:

1. The location of a YSO on the *JHK* color-color diagram is determined to a large extent by its evolutionary state. Protostars, classical T Tauri stars, weak-line T Tauri stars, Herbig AeBe stars, and classical Be stars tend to occupy different regions of color-color space, although overlap of the various types of objects also occurs.
2. The pattern of colors displayed by classical T Tauri stars with near-infrared excesses in the *JHK* color-color diagram can be reproduced very well with standard circumstellar disk models. This finding is consistent with earlier interpretations of their broad-band energy distributions.
3. The near-infrared excesses displayed by AeBe stars, on the other hand, are significantly larger than that which can be produced by standard disk models. However, a wide variety of disk models can fit the observations of AeBe stars provided that both (a) these model disks contain central holes and (b) the physical parameters of the disks and central stars *always* conspire to produce temperatures at the inner edges of the disks in the narrow range 2000–3000 K. Since this temperature range is near the sublimation temperature of interstellar dust, our results suggest that dust is the primary source of opacity in the circumstellar disks around AeBe stars. The data are also consistent with the hypothesis that dust is the primary source of opacity in the disks of classical T Tauri stars. However, because the surface temperatures of these stars are not different enough from the dust destruction temperature, holes in their disks are too small to greatly affect the *JHK* colors of these systems.
4. The AeBe star data also appear to be best fitted by models in which the disks have a significant component of intrinsically generated (accretion?) luminosity.
5. The *JHK* colors of luminous protostars are very similar to those expected from heavily extinguished AeBe stars, and hence AeBe stars may have only very recently emerged from their protostellar envelopes.

Analysis of the *JHK* color-color diagram for young stellar objects indicates that it can be a very useful tool for studying star formation. The reason for this is that observations at wavelengths between 1 and  $2 \mu\text{m}$  probe the environments close to the surface of a YSO and are therefore sensitive to the presence and the structure of any circumstellar material there. In addition, the temperature regime probed by observations at such wavelengths corresponds to that where interstellar dust, a major source of opacity for circumstellar material, is thermally destroyed. It appears that infrared camera observations should be very effective for investigating the natures of obscured clusters and the large populations of YSOs which are embedded in molecular clouds.

We gratefully acknowledge Scott Kenyon for making available his unpublished observations of YSOs in Taurus. We thank Lee Hartmann, Lynne Hillenbrand, and Steve Strom for very stimulating discussions. This research was supported in part by NSF grant AST 8815753.

## APPENDIX

## CORRECTIONS TO MIMIC REALISTIC STELLAR ATMOSPHERES

Because we have used blackbodies to model both the radiation emitted by the central star and its circumstellar disk, our predicted *JHK* colors do not accurately represent the true *JHK* colors of stars with disks. The energy distributions of stars deviate from pure blackbodies because of the nature of stellar opacities. In the wavelength range we are considering the major source of stellar opacity,  $H^-$ , has a minimum (at  $1.6 \mu\text{m}$ ) through which most of the stellar flux absorbed out at shorter (and longer) wavelengths is able to escape the star. This causes the stellar energy distribution to depart increasingly from that of a blackbody for cooler and cooler stars as the peak of the stellar energy distribution moves into the opacity minimum at  $1.6 \mu\text{m}$ . Although differences between blackbody models and real stars begin to be noticeable on the *JHK* color-color diagram for stars with effective temperatures hotter than about 3000 K and cooler than about 7000 K, the departures between predicted and real stellar colors become significant for those stars with temperatures between about 3500 and 5000 K. To illustrate the size of this effect, we plot in Figure 10 the locations on the *JHK* color-color diagram of a standard set of disk models whose central star has an effective temperature (5000 K) corresponding to a K0 main-sequence star. In addition we plot the location of a 5000 K blackbody which represents our model star sans disk. The location of a K0 main-sequence star is also indicated. The arrow indicates the shift needed to correct the model colors to those of a K0 star.

As a first approximation, we can better estimate the colors of a real star-disk system by shifting the colors of all models in a grid by the (same) amount necessary to correct the blackbody colors of the model central star to those of the appropriate main-sequence star. In Figure 11 we plot the distribution of *JHK* colors of two standard disk model grids ( $T_* = 5000 \text{ K}$  [K0] and  $T_* = 6000 \text{ K}$  [G0]) which have been adjusted so that the colors of their central stars correspond to the appropriate main-sequence values. A grid of standard models corresponding to an A0 star (whose colors need negligible adjustment) is also plotted. With these straightforward adjustments, the model grids are more nearly representative of real star-disk systems.

We do expect that a second-order correction is also necessary since the disk atmosphere (which we have modeled as a series of blackbodies) should also deviate from a blackbody at similar cool temperatures. Unfortunately, a quantitative estimate of its magnitude requires detailed modeling of disk atmospheres. This, in turn, requires a detailed knowledge of disk structure, something which at the present time cannot be meaningfully inferred from or constrained by observations or existing theory. Such modeling is certainly beyond the scope of the present paper. Recently, however, Calvet et al. (1992, hereafter CMPD) have attempted to calculate more realistic disk models using a restricted set of assumptions concerning the structure of the disks and a radiative transfer code with appropriate opacities to calculate the emergent energy distribution from a star-disk system. For comparison, we plot in Figure 11 the grid of models CMPD calculated for a 5000 K star which most closely corresponds to our standard models for a similar central star. The adjusted ALS models clearly more closely correspond to the more detailed CMPD models than do the

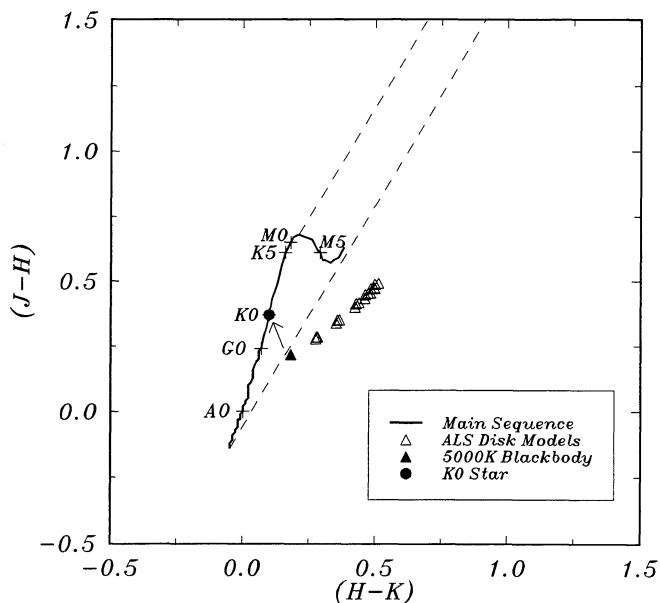


FIG. 10

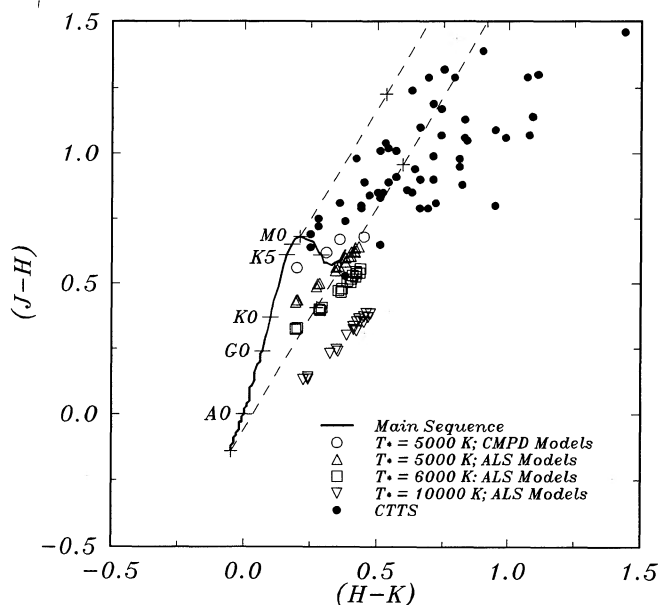


FIG. 11

FIG. 10.—Distribution of the grid of standard disk models corresponding to a 5000 K (K0) central star with  $f_{\text{Disk}} = 0.1$  along with the location of a 5000 K blackbody which corresponds to the colors of the model central star without a disk. Also shown are the locations on the main sequence of stars of various spectral types. The arrow indicates the displacement of the model star colors from those of a real K0 star.

FIG. 11.—A series of standard disk models whose colors have been adjusted to mimic those of more realistic stellar systems by forcing the model central stars to have colors similar to those of main-sequence stars of the same effective temperature. For comparison, a grid of models calculated by Calvet et al. (1992) for a K0 central star using realistic opacities and a radiative transfer code is also plotted. Finally, the observed colors of CTTS are also displayed. The models cannot account for the observed colors of CTTS without the introduction of modest amounts of extinction. In addition, CTTS with the largest infrared excesses can only be fitted by models with large intrinsic disk luminosities.

standard ALS models. However, it is not clear whether the remaining differences in calculated colors are a result of the need for a second-order correction as discussed above or to other differences in assumed disk properties (e.g., accretion rate, flaring, etc.) between the two sets of models. Consequently, it is not all obvious which set of models more closely represents real star-disk systems. Systems whose central stars have lower effective temperatures, in particular stars with spectral types between K5 and M5, will show even greater departures from standard (blackbody) disk models and we have not attempted to consider such systems here.

Finally, in Figure 11 we have plotted the observed colors of CTTS. The adjusted disk models for 5000 and 6000 K central stars do not fit the observations as well as the 3000 K models do (see § 3.1). However, with extinctions between 2 and 5 mag (visual), these models would be able to fit most CTTS. On the other hand, we expect that systems whose central stars have effective temperatures less than 5000 K will be able to match the data with lower amounts of visual extinction (0–3 mag) and are probably more representative of the bulk of CTTS. Even so, CTTS with the largest excesses still clearly require models with large relative disk luminosities as discussed earlier.

## REFERENCES

- Adams, F. C., Emerson, J. P., & Fuller, G. A. 1990, *ApJ*, 357, 606  
 Adams, F. C., Lada, C. J., & Shu, F. H. 1987, *ApJ*, 321, 788 (ALS)  
 ———. *ApJ*, 326, 865 (ALS88)  
 Adams, F. C., & Shu, F. H. 1986, *ApJ*, 308, 836  
 Alexander, D. R., Johnson, H. R., & Rympa, R. L. 1983, *ApJ*, 272, 773  
 Ashok, N. M., Bhatt, H. C., Kulkarni, P. V., & Joshi, S. C. 1984, *MNRAS*, 211, 471  
 Barsony, M., Shombert, J. M., & Kis Halas, K. 1991, *ApJ*, 379, 221  
 Beall, J. H. 1987, *ApJ*, 316, 227  
 Beckwith, S. V. W., Sargent, A. I., Chini, R. S., & Gusten, R. 1990, *AJ*, 99, 924  
 Calvet, N., Magris, G. C., Patino, A., & D'Alessio, P. 1992, *Rev. Mexicana Astron. Af.*, in press (CMPD)  
 DePoy, D. L., Lada, E. A., Gatley, I., & Probst, R. 1990, *ApJ*, 356, L55  
 Elston, R., ed. 1991, *Astrophysics with Infrared Arrays* (ASP Conf. Ser. 14)  
 Emerson, J. P., in *The Formation and Evolution of Low Mass Stars*, ed. A. K. Dupree & M. T. U. T. Largo (Dordrecht: Kluwer), 193  
 Finkenzeller, U., & Mundt, R. 1984, *A&AS*, 55, 109  
 Gatley, I., Merrill, K. M., Fowler, A. M., & Tamura, M. 1991, in *Astrophysics with Infrared Arrays* (ASP Conf. Ser. 14), 230  
 Gezari, D. Y., Schmitz, M., & Mead, J. M. 1987, *Catalog of Infrared Observations* (NASA Pub. 1196)  
 Gehrz, R. D., Hackwell, J. A., & Jones, T. J. 1974, *ApJ*, 191, 675  
 Herbig, G. H., & Bell, R. 1988, *Lick Obs. Bull.*, 1111  
 Hillenbrand, L., Strom, S. E., Urba, F. J., & Keene, J. 1992, in preparation  
 Hughes, J. 1989, Ph.D. thesis, Queen Mary College  
 Hyland, A. R., 1981, in *IAU Symp. 96, Infrared Astronomy*, ed. C. G. Wynn-Williams & D. P. Cruikshank (Dordrecht: Reidel), 125  
 Johnson, H. L. 1966, *ARA&A*, 4, 193  
 Kenyon, S. J., & Hartmann, L. W. 1987, *ApJ*, 323, 714  
 Kenyon, S. J., & Hartmann, L. W. 1992, in preparation  
 Koornneef, J. 1983, *A&A*, 128, 84  
 Lada, C. J. 1987, in *IAU Symp. 115, Star Forming Regions*, ed. M. Peimbert & J. Jugaku (Dordrecht: Reidel), 1  
 ———. 1991, in *The Physics of Star Formation and Early Stellar Evolution*, ed. C. J. Lada & N. D. Kylafis (Dordrecht: Kluwer), 329  
 Lada, C. J., De Poy, D. L., Merrill, M., & Gatley, I. 1991, *ApJ*, 374, 533  
 Lada, C. J., & Shu, F. H. 1990, *Science*, 248, 1222  
 Lada, E. A., De Poy, D. L., Evans, N. J., & Gatley, I. 1991, *ApJ*, 371, 171  
 Lamers, H. J. G. L. 1987, in *IAU Colloq. 92, Physics of Be Stars*, ed. A. Slettebak & T. P. Snow (Cambridge: Cambridge Univ. Press), 219  
 McGregor, P. J., Persson, S. E., & Cohen, J. G. 1984, *ApJ*, 286, 609  
 Mendoza, E. E. V. 1987, in *IAU Colloq. 92, Physics of Be Stars*, ed. A. Slettebak & T. P. Snow (Cambridge: Cambridge Univ. Press), 219  
 Natta, A., Palla, F., Butner, H. M., Evans, N. J., & Harvey, P. M. 1992, *ApJ*, 391, in press  
 Palla, F., & Stahler, S. W. 1991, *ApJ*, 360, L47  
 Rucinski, S. M. 1985, *AJ*, 90, 2321  
 Shu, F. H. 1977, *AJ*, 214, 488  
 Shu, F. H., Adams, F. C., & Lizano, S. 1987, *ARA&A*, 25, 23  
 Strom, S. E., Keene, J., Edwards, S., Hillenbrand, L., Strom, K., Gauvin, L., & Condon, G. 1992, preprint  
 Wynn-Williams, C. G. 1982, *ARA&A*, 20, 587  
 Wynn-Williams, C. G., & Becklin, E., ed. 1987, *Infrared Astronomy with Arrays* (Honolulu: University of Hawaii, Institute for Astronomy)  
 Zinnecker, H., McCaughrean, M., & Wilking, B. A. 1992, in *Protostars and Planets III*, ed. G. Levy & J. Lunine (Tucson: Univ. of Arizona Press), in press